

Experimental demonstration of ray-optical refraction with confocal lenslet arrays

Johannes Courtial,^{1,*} Blair C. Kirkpatrick,¹ Eric Logean,² and Toralf Scharf²

¹*School of Physics & Astronomy, University of Glasgow, Glasgow G12 8QQ, UK*

²*Optics and Photonics Technology Laboratory, Ecole Polytechnique Fédérale de Lausanne, Rue A.-L. Breguet 2, 2000 Neuchâtel, Switzerland*

*Corresponding author: Johannes.Courtial@glasgow.ac.uk

Received August 11, 2010; revised October 22, 2010; accepted November 2, 2010;
posted November 9, 2010 (Doc. ID 131492); published November 30, 2010

We observe imaging through windows comprising pairs of confocal lenslet arrays that have different focal lengths but that are otherwise identical. Image space is stretched in the longitudinal direction only. Such windows are examples of METATOYS, optical components that can change light-ray direction in ways that appear wave-optically forbidden. © 2010 Optical Society of America

OCIS codes: 160.1245, 240.3990.

Two lenslet, or microlens, arrays that share a common focal plane and have different focal lengths “refract” (that is, redirect) light rays in a manner similar to the interface between optical media with different refractive indices [1]. More precisely, this is true for light rays that pass through corresponding lenslets, that is, through lenslets that share a common optical axis; light rays for which this is not the case are refracted differently [2]. Such confocal lenslet arrays (CLAs) correspond to a refractive-index ratio $\eta = n_2/n_1$, where [1]

$$\eta = -\frac{f_2}{f_1}, \quad (1)$$

and f_1 and f_2 are the focal lengths of the two lenslet arrays. The parameter η can be positive or negative.

Planar CLAs image all space, such that the transverse magnification is always +1 and the longitudinal magnification is always η [1,3,4]—image space is stretched in the longitudinal direction by a factor η . These imaging characteristics are quite unlike those of a single lens. In combination with those of an ideal thin lens, they represent the most general object-image-space mapping that can be performed by any infinite light-ray-direction-changing window that images all space [5].

CLAs can be seen as an example of a METATOY (metamaterial for rays), a class of optical windows with analogies with metamaterials [6]. What makes METATOYS special is that they can perform refraction that leads to light-ray fields that have no wave-optical analog, and that are, therefore, even beyond the reach of metamaterials. Another example of METATOY refraction, local light-ray rotation [7,8], can be formally described as acting like the interface between materials with a *complex* refractive-index ratio [9].

CLAs in which both arrays have the same focal length (i.e., $\eta = -1$), have long been used for 1:1 imaging of large areas [10,11]. They can also be used to turn the pseudoscopic images produced by integral imaging into orthoscopic images [12]. They do this by being essentially another integral-imaging setup [13]: one lenslet array is the camera and produces the intensity distribution corresponding to the integral image in the common focal plane (this also goes by the name “plenoptic camera” [14,15]);

the other lenslet array is for viewing the integral image (this is one of the techniques of producing stereo images in three-dimensional displays [16]). If the lenslet arrays are rotated with respect to each other such that they still share a common focal plane, this results in an array of rotated and reduced-size images [17]; such a setup is called a “moiré magnifier.” If the lenslet arrays have different pitch, the combination has a few of the properties of a lens [18] and is called a “Gabor superlens” [19].

We have used microfabrication technology [20] to manufacture several lenslet arrays with the same array pattern and pitch but with two different focal lengths, 0.30 and 0.53 mm. This allows us to realize CLAs with three different values of η , namely, $\eta = -0.57$, $\eta = -1.7$, and the case $\eta = -1$. We present here experiments demonstrating one of the key properties of CLAs: imaging that stretches the longitudinal direction. Our experiments expand on a previous experiment that used CLAs with $\eta \neq 1$ to image a planar mask with transverse magnification +1 and unequal image and object distances [4].

At the heart of our experiment are lenslet arrays. Each lenslet array consists of paraboloid bumps of red-tinted, transparent resin (AZ9260, MicroChemicals GmbH, Germany, refractive-index $n = 1.67$) on a 100 mm diameter fused-silica wafer (some wafers were of thickness 0.55 mm, others 0.3 mm). The resin structure was fabricated by photolithography and resist processing (reflow) [20]. Each lenslet in the array has a diameter of 250 μm ; each array consists of hexagonally packed lenslets covering a disk of diameter 79 mm.

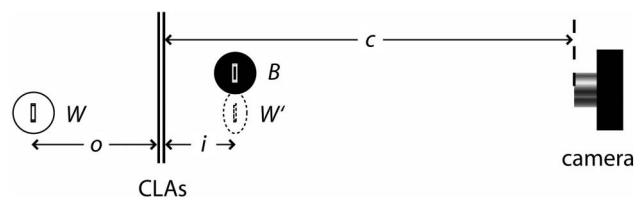


Fig. 1. Schematic top view of the experimental setup for Figs. 2 and 4. B , W , and W' are, respectively, the black knight, the white knight, and the image of the white knight formed by the CLAs. c , o , and i are the camera, object, and image distances, respectively. The sketch is not to scale.

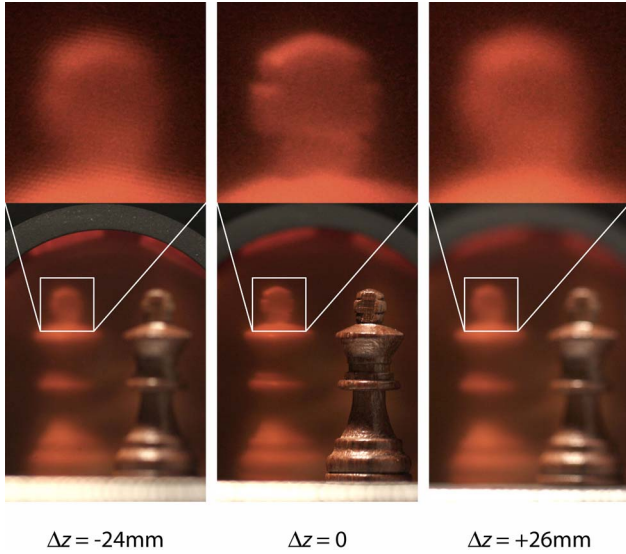


Fig. 2. (Color online) Confirmation of the image position through focusing. The image of the white chess piece created by the CLAs ($\eta = -0.57$) goes in and out of focus together with the black chess piece as the position of the focus plane changes. The focusing plane is a distance Δz in front of the black chess piece; the measured object and image distances are $o = 70$ mm and $i = 34$ mm ($i/o = 0.49$). The photos shown here are from a movie (Media 1).

We require fine adjustment of the two lenslet arrays' relative tilt, separation, and transverse position. This is achieved by attaching the arrays to suitable 50 mm diameter optical mounts. The lenslet arrays are mounted such that the resin structures of the two lenslet arrays face each other.

Our particular choice of mounts has the disadvantage of reducing the visible area of the lenslet arrays. However, the area remains sufficiently large to observe the

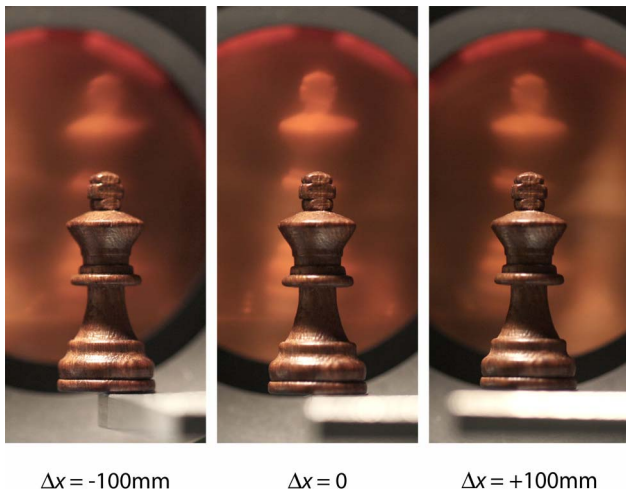


Fig. 3. (Color online) Horizontal parallax. As the camera is moved left and right (a distance Δx out of the default position), the image (produced by CLAs with $\eta = -0.57$) of the white chess piece does not move relative to the black chess piece. Out-of-focus additional "ghost" images [2] of the white knight are visible, most notably in the rightmost frame to the right of the black knight. The measured object and image distances are, respectively, $o = 70$ mm and $i = 34$ mm ($i/o = 0.49$). The photos are part of a movie (Media 2).

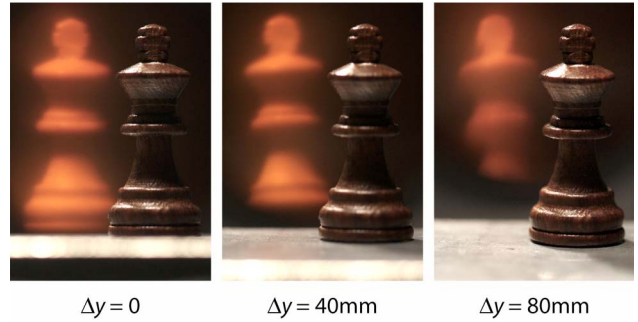


Fig. 4. (Color online) Vertical parallax. As the camera is moved upward (Δy is the height above the default position), the image of the white chess piece does not move relative to the black chess piece. When seen from above ($\Delta y > 0$), the image of the white chess piece appears to be seen from below; this is due to the image being pseudoscopic, and, therefore, in this case, "hollow" (like the bust in the hollow-bust optical illusion [21]). Here this effect is enhanced because the depth of the image is stretched. This is particularly apparent in the corresponding movie (Media 3). The pictures were taken using CLAs with $\eta = -1.7$; measured object and image distances are $o = 56$ mm and $i = 100$ mm, respectively ($i/o = 1.8$).

images produced by the CLAs directly, using stereopsis, often to striking effect.

We place a white chess piece behind the CLAs and a black chess piece in front. We move one or both of the chess pieces such that the black piece is the same distance in front of the CLAs as the image of the white piece; we check this using focusing and parallax. The distance of the white and black chess piece behind and in front of the CLAs is then, respectively, our measured object distance, o , and image distance, i (Fig. 1). Because image space is stretched longitudinally by a factor η with respect to object space, and the plane of the CLA is imaged into itself, we expect the ratio of image and object



Fig. 5. (Color online) Pseudoscopic imaging. Two white chess pieces at different object distances ($o_1 = 76$ mm and $o_2 = 90$ mm) are being imaged by CLAs ($\eta = -1.7$). For comparison, two black chess pieces have been placed in the corresponding image planes ($i_1 = 140$ mm and $i_2 = 150$ mm). From the camera position (480 mm in front of the CLAs), the images of the two white chess pieces overlap, and so do the two black chess pieces. However, whereas the black chess piece in front (the knight) obscures the one behind (the pawn), the image behind (of the white pawn) obscures that in front.

distance to be

$$\frac{i}{o} = -\eta. \quad (2)$$

Unless otherwise stated, all photos are taken with a 100 mm lens at f -number $f/2.8$, from a distance 500 mm in front of the CLAs. The camera is approximately positioned on the axis through the CLA's center and perpendicular to it. Respectively using focusing, horizontal parallax, and vertical parallax, Figs. 2 (Media 1), 3 (Media 2), and 4 (Media 3) confirm the image is in the expected position.

As $\eta < 0$ in our experiments, space is inverted longitudinally and the images are pseudoscopic. Figures 4 and 5 demonstrate two of the counterintuitive properties of this pseudoscopic imaging.

The CLAs investigated here suffer from field-of-view limitations that were previously investigated theoretically [2]. In our case, these limitations show up as additional ("ghost") images, visible in Fig. 3. We do not investigate them here in any detail, but we note that it is possible to increase the field of view with the help of a field lens in the common focal plane, as previously demonstrated for CLAs with $\eta = -1$ [12] and for the Gabor superlens [22].

Our experiment shows that CLAs work as expected. We were positively surprised by the image quality that can be achieved. During alignment, we observed effects very closely related to the moiré magnifier [17] but subtly altered by the difference in focal lengths between the two lenslet arrays. In the future, we intend to investigate these in more detail.

B. C. Kirkpatrick acknowledges funding through an Engineering and Physical Sciences Research Council (EPSRC) Vacation Bursary. Many thanks to Irène Philipoussis Fernandez for her technical expertise and to Dr. Graham Gibson for his help with the experiment.

References

1. J. Courtial, *New J. Phys.* **10**, 083033 (2008).
2. J. Courtial, *Opt. Commun.* **282**, 2634 (2009).
3. M. C. Hutley and R. F. Stevens, in *Microlens Arrays*, M. C. Hutley, ed., IOP Short Meetings Series No. 30 (Institute of Physics, 1991), pp. 147–154.
4. R. F. Stevens and N. Davies, *J. Photogr. Sci.* **39**, 199 (1991).
5. J. Courtial, *Opt. Commun.* **282**, 2480 (2009).
6. A. C. Hamilton and J. Courtial, *New J. Phys.* **11**, 013042 (2009).
7. A. C. Hamilton, B. Sundar, J. Nelson, and J. Courtial, *J. Opt. A* **11**, 085705 (2009).
8. M. Blair, L. Clark, E. A. Houston, G. Smith, J. Leach, A. C. Hamilton, and J. Courtial, *Opt. Commun.* **282**, 4299 (2009).
9. B. Sundar, A. C. Hamilton, and J. Courtial, *Opt. Lett.* **34**, 374 (2009).
10. R. H. Anderson, *Appl. Opt.* **18**, 477 (1979).
11. R. Völkel, H. P. Herzig, P. Nussbaum, R. Dändliker, and W. B. Hügler, *Opt. Eng.* **35**, 3323 (1996).
12. R. F. Stevens and T. G. Harvey, *J. Opt. A* **4**, S17 (2002).
13. G. Lippmann and C. R. Hebd, *Acad. Sci.* **146**, 446 (1908).
14. T. Adelson and J. Y. A. Wang, *IEEE Trans. Pattern Anal. Machine Intell.* **14**, 99 (1992).
15. R. Ng, M. Levoy, M. Brédif, G. Duval, M. Horowitz, and P. Hanrahan, "Light field photography with a hand-held plenoptic camera," Stanford Tech. Report CTSR 2005-02 (2005).
16. T. Okoshi, *Proc. IEEE* **68**, 548 (1980).
17. M. C. Hutley, R. Hunt, R. F. Stevens, and P. Savander, *Pure Appl. Opt.* **3**, 133 (1994).
18. D. Gabor, "Improvements in or relating to optical systems composed of lenticules," UK patent 541,753 (1940).
19. C. Hembd-Sölner, R. F. Stevens, and M. C. Hutley, *J. Opt. A* **1**, 94 (1999).
20. P. Nussbaum, R. Völkel, H. P. Herzig, M. Eisner, and S. Haselbeck, *Pure Appl. Opt.* **6**, 617 (1997).
21. W. Dultz, *Appl. Opt.* **23**, 200 (1984).
22. J. Duparré, P. Schreiber, A. Matthes, E. Pshenay-Severin, A. Bräuer, A. Tünnermann, R. Völkel, M. Eisner, and T. Scharf, *Opt. Express* **13**, 889 (2005).